

# Mathematical modelling of the 3-D mixing in an induction plasma reactor

ZOUHIR NJAH,<sup>†</sup> JAVAD MOSTAGHIMI<sup>‡</sup> and MAHER BOULOS<sup>†</sup>

<sup>†</sup> Plasma Technology Research Centre (CRTP), University of Sherbrooke, Sherbrooke, Québec, Canada, J1K 2R1

<sup>‡</sup> Department of Mechanical Engineering, University of Toronto, Toronto, Ontario, Canada, M5S 1A5

(Received 8 December 1992 and in final form 4 May 1993)

**Abstract**—In this paper we have formulated a three-dimensional laminar model for the prediction of the mixing pattern of single and multiple cold jets with a transverse plasma flow. In the analysis and modelling of this problem, the situation has often been approximated by two-dimensional models in which the multiple jets are approximated by a circular slot. The validity of such an approximation is the subject of the present investigation.

## 1. INTRODUCTION

MIXING of cold jets introduced in a thermal plasma reactor is of great importance in plasma chemistry. The success of a plasma chemical process depends to a large extent on the knowledge of the flow, temperature and concentration fields in the reaction zone. In a radio frequency (r.f.) induction plasma reactor, one of the reactants is often injected centrally through a water cooled probe, while the second reactant, or product quench medium, is injected laterally through single or multiple ports. A review of the subject has been reported by Laflamme *et al.* [1]. The approach has also been used by Soucy [2] for the synthesis of high purity ultrafine powders of silicon nitride through the reaction of silicon tetrachloride with ammonia. In this case a SiCl<sub>4</sub>/Ar gaseous mixture was axially injected into the center of the discharge while NH<sub>3</sub> was radially injected into the plasma jet at the exit of the induction plasma torch. The result showed that the quality of the silicon nitride powder obtained depends strongly on the mixing conditions in the reaction zone.

Soucy *et al.* [3, 4] reported an experimental study of the mixing pattern in an induction plasma reactor for both axial and radial injection modes. The results obtained for the Ar/N<sub>2</sub> system under atmospheric and low pressure conditions underline the increasing difficulty of gas mixing under plasma conditions compared to that at room temperature. The results also show that in the radial injection mode, the injection gas velocity has an important influence on the mixing length which was found to be typically of the order of two tube diameters from the point of injection.

Mathematical modelling studies have also been reported in the literature dealing with the problem of gas mixing in both direct current (d.c.) and radio frequency (r.f.) induction plasma reactors. These have often resorted to a two-dimensional simplification of the flow pattern in the reactor chamber [5] through

the approximation of the lateral injection ports by a narrow cylindrical slot. While such an approximation might be valid when a large number of injection ports are used, it is not necessarily representative of optimum mixing configuration to be used.

A large number of experimental, analytical and computational investigations dealing with jets discharging into transverse streams have been carried out under isothermal and relatively low temperature flow conditions. Experimental investigations of the behavior of jets issuing normally into a cross stream have been mostly devoted to measuring the jet trajectory, jet spread, mean velocity, temperature and pressure fields. Jordison [6], Keffer and Baines [7], Keffer [8], Platten and Keffer [9], and Moussa *et al.* [10] studied the general features of a jet injected normally into a cross stream and presented data for the jet trajectory. Patrick [11] reported velocity and concentration measurements of the mixing of a round turbulent jet with a transverse main stream. Gelb and Martin [12], Wu *et al.* [13], and McMahon and Mosher [14] made measurements of the pressure fields resulting from the interaction of a jet with a cross stream. Margason [15], McMahon *et al.* [16], and Mikolowsky and McMahon [17] studied the interference effects associated with a jet in a cross stream. Ramsey [18], Ramsey and Goldstein [19], and Campbell and Schetz [20] studied the interaction between heated jets and a cross stream. Kamotani and Greber [21] reported measurements of the velocity, temperature, and turbulence intensity fields of jets in cross flows. Rudinger [22] measured the penetration of side jets introduced in a cross flowing stream through a narrow slot. Chassing *et al.* [23] made measurements of the flow characteristics of jets in the presence of a cross stream. Bergeles *et al.* [24] studied the flow field in and around a circular air jet injected normal to a main stream. Crabb *et al.* [25] used laser Doppler anemometry to measure the velocity in the near field of a round jet normal to a cross flow. Raja-



i.d. induction plasma torch, 425 mm long. Calculations are carried out for an argon plasma flow in which a lateral helium jet is introduced, 208 mm downstream the entrance section of the torch, from either single or multiple ports or a cylindrical annular slot. In order to maintain a constant auxiliary gas injection velocity ( $8.35 \text{ m s}^{-1}$ ), in all these cases, the total injection area is fixed at  $16 \text{ mm}^2$ . This corresponds to a single 4.51 mm i.d. injection port, or two 3.19 mm i.d. ports, or four 2.26 mm i.d. ports and so on. For the case of the circular slot, the width of the annular slot was 0.1 mm.

Since the jet(s) interaction with the main is mostly limited to the region downstream of the injection point(s), the model formulation was carried out in two steps as follows:

The first involved the full flow and temperature fields in the r.f. plasma torch in the absence of any lateral jet injection. The flow configuration in this case was represented by a standard 2-D formulation as described by Mostaghimi *et al.* [41, 42]. The approach is based on the solution of the 2-D continuity, momentum and energy equations simultaneously with the corresponding simplified form of Maxwell's equations for the electromagnetic fields. Details of the basic assumptions, governing equations and numerical method used in this stage are given in refs. [41, 42].

The results obtained from the 2-D model were next used as input conditions for the 3-D computations. As shown in Fig. 1 the computation domain in this case did not include the induction coil. The upstream boundary was located at 175 mm from the main entrance of the torch. The injection section of the lateral jet(s) was 33 mm farther downstream. The total 3-D computation domain was 250 mm long as identified by the dotted line in Fig. 1.

Because of the absence of the electromagnetic fields in this zone, the model could be limited to the solution of the corresponding continuity, momentum, energy and mass transfer equations using the following basic assumptions:

- (1) Steady, laminar and incompressible fluid flow.
- (2) 3-D Cartesian ( $x, y, z$ ) system of coordinates.
- (3) Negligible viscous dissipation and gravity effects.
- (4) Negligible radiative energy losses from the plasma.

## 2.2. Governing equations

Based on the above assumptions, the 3-D continuity, momentum, energy and concentration equations can be written in vector notation as follows:

continuity equation:

$$\vec{\nabla} \cdot (\rho \vec{u}) = 0 \quad (1)$$

momentum equations:

$$\rho \vec{u} \cdot (\vec{\nabla} \vec{u}) = -\vec{\nabla} p - \vec{\nabla} \cdot \vec{\tau} \quad (2)$$

energy equation:

$$\rho \vec{u} \cdot (\vec{\nabla} h) = \vec{\nabla} \cdot \left( \frac{k}{c_p} \vec{\nabla} h \right) \quad (3)$$

concentration equation:

$$\rho \vec{u} \cdot (\vec{\nabla} c) = \vec{\nabla} \cdot (\rho D \vec{\nabla} c) \quad (4)$$

where  $\vec{u}$ : ( $u, v, w$ ) is the velocity vector,  $\rho$  is the density,  $\vec{\tau}$  is the viscous shear stress,  $p$  is the pressure,  $h$  is the enthalpy,  $k$  is the thermal conductivity,  $c_p$  is the specific heat at constant pressure,  $c$  is the concentration (mass fraction) of the injected gas and  $D$  is the binary diffusion coefficient.

The thermodynamic and transport properties for argon and nitrogen were obtained as function of temperature from ref. [43]. Mixture rules [44] were employed for the calculation of the thermodynamic and transport properties as functions of composition; the density of a mixture of gases A and B is obtained, for example, as follows:

$$\rho = c\rho_A + (1-c)\rho_B \quad (5)$$

where  $\rho$  is the density of the mixture,  $c$  is the mass fraction of A in the mixture,  $\rho_A$  and  $\rho_B$  are, respec-

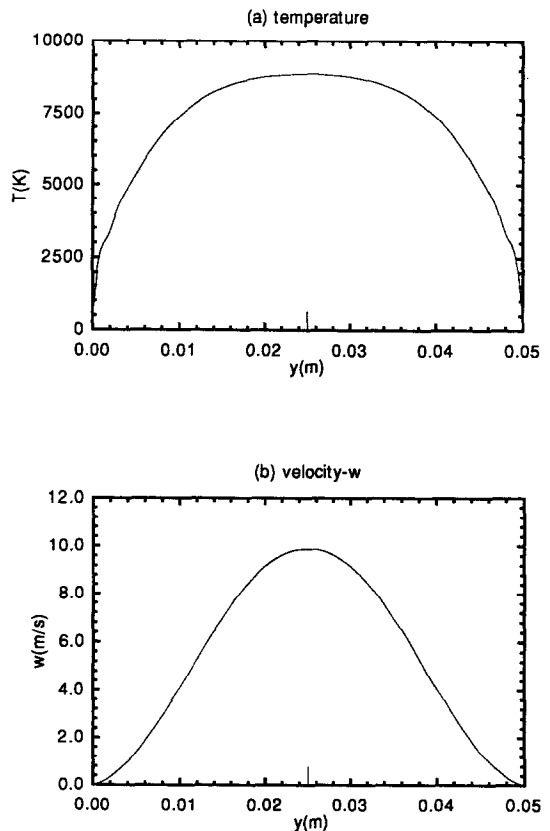


FIG. 2. Temperature (a) and velocity (b) profiles at the inlet plane of the computation domain ( $z = 0$ ).

tively, the density of A and B gases under the local mixing conditions.

2.3. *Boundary conditions*

Because of the differences in the various configurations studied, the boundary conditions are presented here only for the numerical treatment of a single jet with a cross-flowing plasma stream (Fig. 1). In this case equations (1)–(4) are subject to the following boundary conditions:

- Entrance of the main stream,  $z = 0$

At the entrance of the plasma flow, the velocity and temperature are calculated for a 5 kW, 3 MHz, 50

mm standard r.f. plasma torch [41, 42]. The inlet temperature and velocity of the plasma stream are given in Fig. 2. These were obtained by the solution of the appropriate modelling code described in refs. [41, 42].

- Entrance conditions of the side jet,  $x = 0, y = 0, z = 33 \text{ mm}$

$$T_i = 350 \text{ K}, \quad v_i = 8.35 \text{ m s}^{-1}, \quad u = w = 0, \quad c = 1.0.$$

- Plane of symmetry,  $x = 0$

$$u = \frac{\partial v}{\partial x} = \frac{\partial w}{\partial x} = \frac{\partial h}{\partial x} = \frac{\partial c}{\partial x} = 0.$$

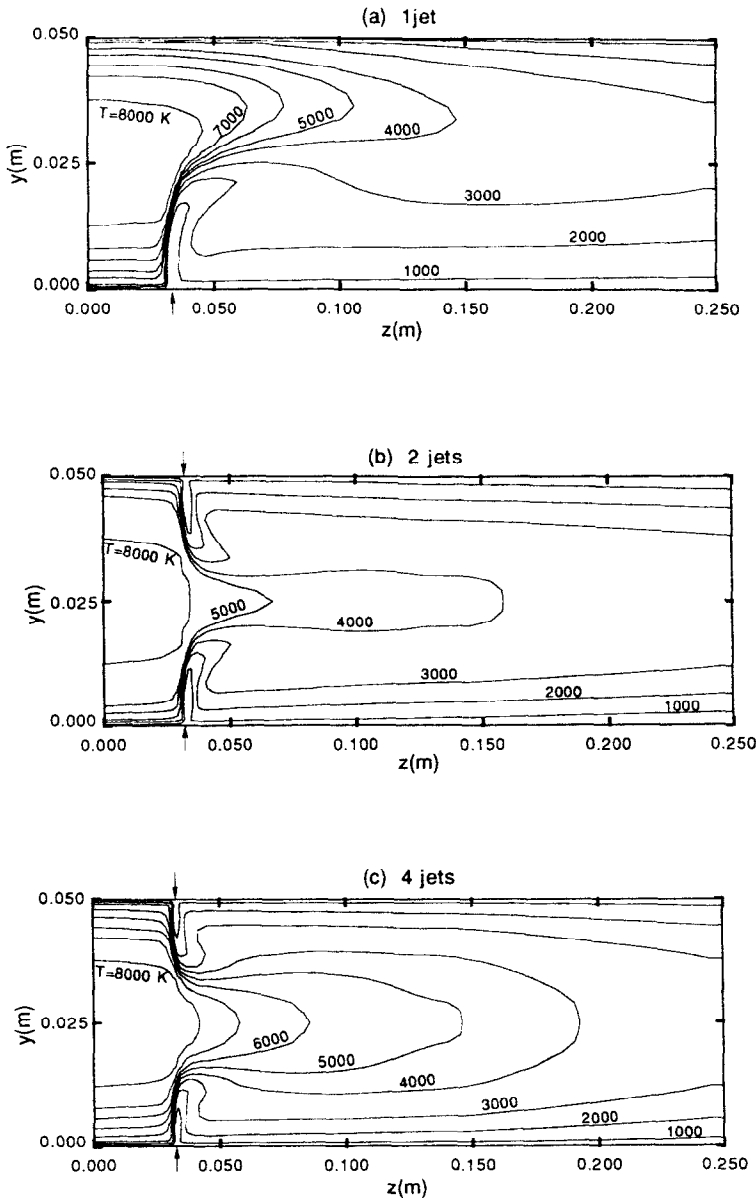


FIG. 3. Temperature fields on the plane of symmetry for single and multiple jets injection.

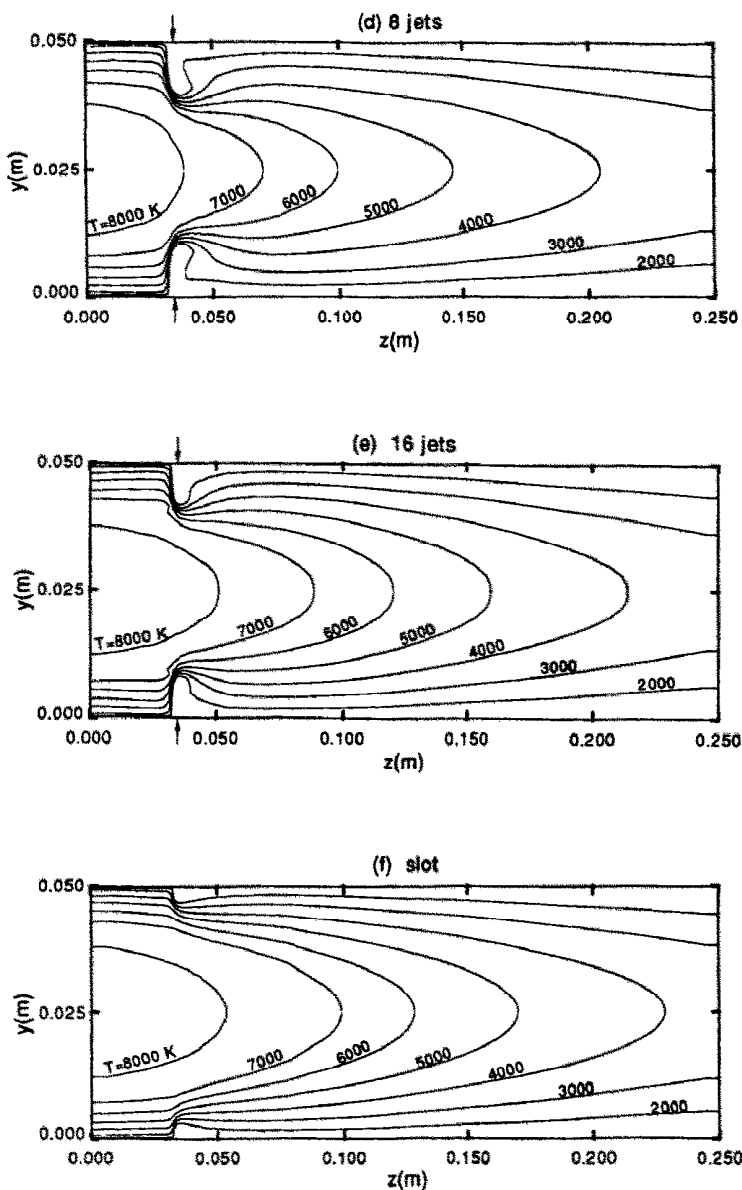


FIG. 3.—Continued.

- Solid wall, along the circular periphery of the plasma confinement tube

$$T = 350 \text{ K}, \quad u = v = w = 0, \quad \frac{\partial c}{\partial x} = \frac{\partial c}{\partial y} = 0.$$

- Exit plane,  $z = 250 \text{ mm}$

At the exit plane the gas temperature, velocity and concentration fields are not known a priori. However, if the exit Peclet number ( $Pe = Re \cdot Pr$ ), is sufficiently large, one can assume that the axial derivatives of the velocity, temperature and concentration are equal to zero.

$$\frac{\partial u}{\partial z} = \frac{\partial v}{\partial z} = \frac{\partial(\rho w)}{\partial z} = \frac{\partial h}{\partial z} = \frac{\partial c}{\partial z} = 0.$$

#### 2.4. Solution procedure

The solution procedure is based on the SIMPLE algorithm (Semi-Implicit Method for Pressure Linked Equations) described in ref. [45] for three-dimensional elliptic situations. The important features of the procedure are described in ref. [46].

Calculations were carried out with a non-uniform grid spacing, the grid points were arranged so that they are densely packed close to the injection point(s) where the gradients are the highest. For locations away from the injection section the grid spacing is

gradually increased. In most cases, the computational field was covered by  $22 \times 32 \times 52$  grid nodes in the  $x$ ,  $y$  and  $z$  directions, respectively. Convergence was reached when, from one iteration to the next, the change in the value of each of the dependent variables was less than 0.001% of the maximum value of its field. A solution required close to 2000 iterations which could be carried out on an IBM RISC 530/6000 computer in about 20 h.

Preliminary tests were performed to explore the grid dependency of the numerical results. The grids in each direction were refined until negligible differences (less than 1%) were found between predictions of the two finer spacing. A grid with  $22 \times 32 \times 52$  nodes in the  $x$ ,  $y$  and  $z$  directions, respectively, was sufficient to insure our numerical solutions to be grid-independent for all

the studied cases. Our results showed that we need a fine grid distribution only in a relatively small region around the section of injection. Thus increasing the number of grid nodes in the longitudinal direction with increasing the number of jets has negligible influence on the numerical solution. In addition, the computational domain, half of the flow field in the single jet case, was reduced to quarter of the flow field for the 2, 4, 8 and 16 jets cases.

Since the computer program used in this study was written for a Cartesian grid, the cylindrical configuration of the duct for the main stream was approximated by rendering inactive 'blocking-off' the control volumes outside the flow domain. The blocking-off operation consists of establishing known values of the relevant dependent variables. In our case

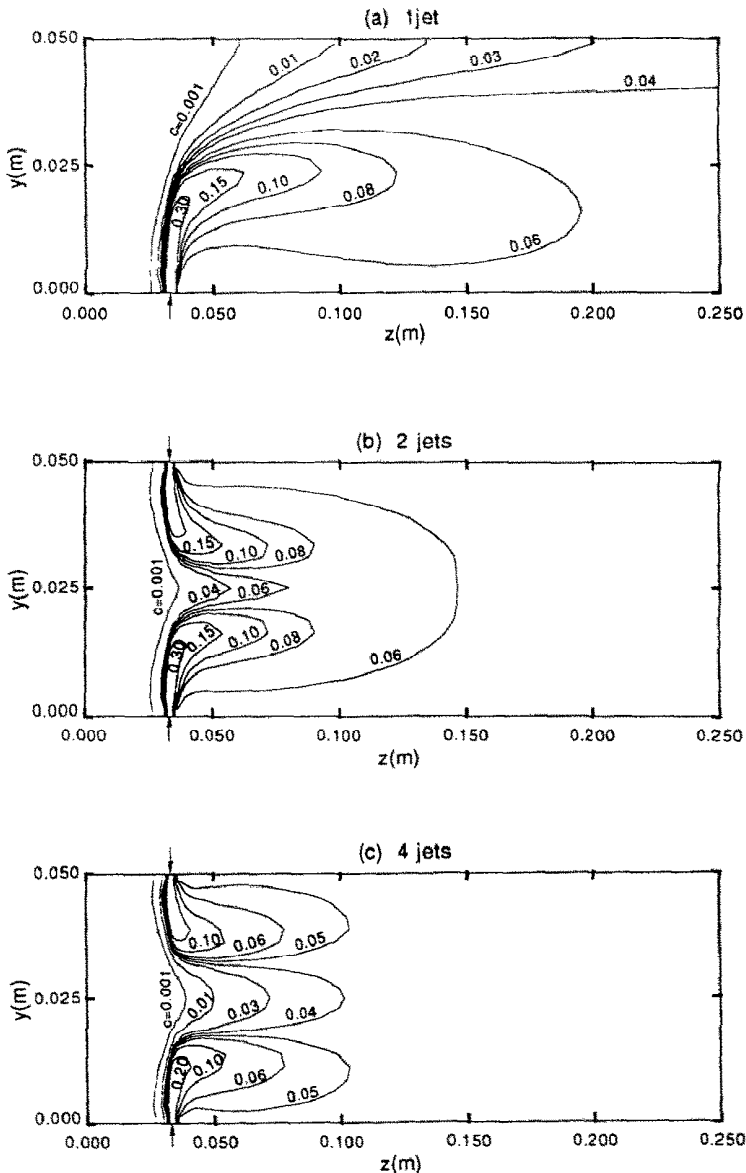


FIG. 4. Helium mass fraction distributions on the plane of symmetry for single and multiple jets injection.

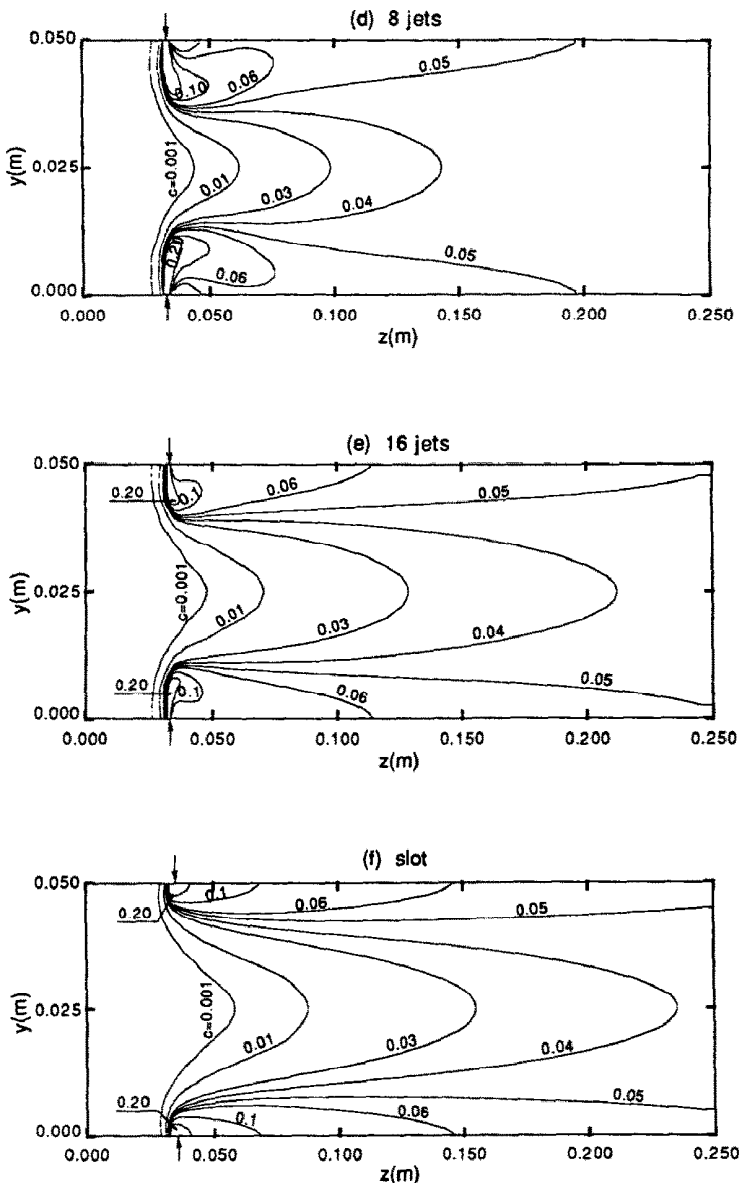


FIG. 4.—Continued.

the inactive region is handled as a stationary solid. In other words the boundary conditions described for the solid wall stands for the inactive region.

The SIMPLE algorithm is usually used to solve incompressible flows with constant density. The incompressible nature of r.f. plasma flows was demonstrated in ref. [46].

On the question of artificial diffusion, Njah *et al.* [46] showed that only a small number of grids, around the injection section, are affected by this numerical problem; the great majority of the control volumes in the flow are parallel to grid-lines giving rise to a negligible artificial diffusion.

### 2.5. Model calibration

In order to calibrate the model, its predictions were first tested against experimental data available in a

cold flow situation in which a nitrogen side jet is injected into an argon main stream. The results presented in ref. [46] showed good agreement between the measured and predicted concentration fields in the immediate mixing zone. This agreement is, however, less satisfactory in the fringe of the jet due to experimental limitations related to probe interference with the flow pattern and the difficulty in maintaining isokinetic sampling conditions at all times.

## 3. RESULTS AND DISCUSSION

Results are presented for the mixing characteristics of helium cold jets injected laterally into an atmospheric plasma cross flow. A comparison is made between mixing patterns of 1, 2, 4, 8, or 16 jets and an annular slot injection downstream of a r.f. inductively

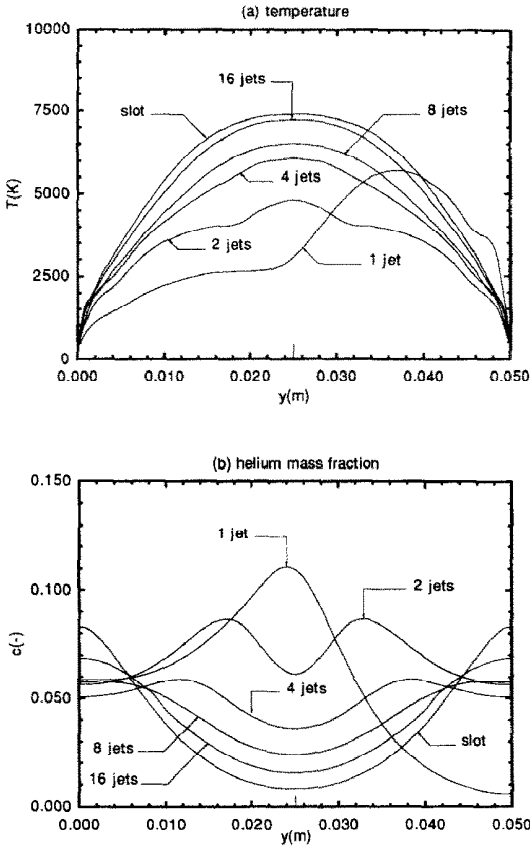


FIG. 5. Temperature (a) and helium mass fraction (b) profiles on the plane of symmetry at one tube diameter downstream of the point of injection ( $z - z_1 = 50$  mm).

coupled plasma torch. The inlet temperature and velocity profiles of argon are calculated for a 5 kW, 3 MHz, 50 mm standard r.f. plasma torch [41, 42]. The total argon flow rate is 20 slpm ( $Q_1 = 2$  slpm,  $Q_2 = 3$  slpm,  $Q_3 = 15$  slpm). The mass ratio of helium to the total argon mass flow rate is maintained at 0.05. Since the injection surface was kept constant, the lateral gas injection velocity was also fixed at  $8.35 \text{ m s}^{-1}$  throughout the study.

Before comparing the mixing characteristics

between single and multiple jets with a transverse plasma stream, it is worth describing the main features of the flow field associated with a jet in a cross flow. Figure 3(a) shows the temperature distribution in the plane of symmetry obtained with a single jet. From this figure, one can see that at the source, the jet trajectory is almost unaffected by the presence of the main stream. In this region, the obstructing jet decelerates the plasma stream at its upstream surface giving rise to a region of positive pressure and forces the plasma stream to accelerate around the obstruction caused by the jet. Moreover, the main stream forces the jet, subject to intense shear stress, to deflect and a reverse flow region, called the wake-jet region, appears downstream the injection point. This region of negative pressure promotes rapid mixing between the two streams.

Temperature distributions in the plane of symmetry, obtained with 1, 2, 4, 8 and 16 jets, are shown in Figs. 3(a)–(e), respectively. From a comparison of each of these temperature fields with that of the slot injection (Fig. 3(f)), which is the result of a 2-D model, it is obvious that substantial differences can be observed for the 1, 2, and 4 jets cases. Indeed a circular slot is not even a perfect representation of the 16 points injection case, the differences in the resultant temperature fields are, however, sufficiently small to justify the use of a 2-D model in this case, considering the substantial simplification of the computation compared to that required for the 3-D model. The results show, however, that the use of a 2-D model would be far from satisfactory for any of the smaller number of injection ports, certainly for those corresponding to 1, 2 and 4 ports. Figure 3 also reveals interesting information on the flow character in the jet(s)-wake region(s); for an increased number of jets, the fluid temperature near the wall is significantly affected by the temperature of the jet fluid while that is unlikely to happen for a reduced number of jets. The former case is in effect that which occurs in discrete film cooling, except that the injection velocity may be slightly lower for effective cooling processes.

A comparison of helium mass fraction distributions in the plane of symmetry, obtained with 1 and 2 injec-

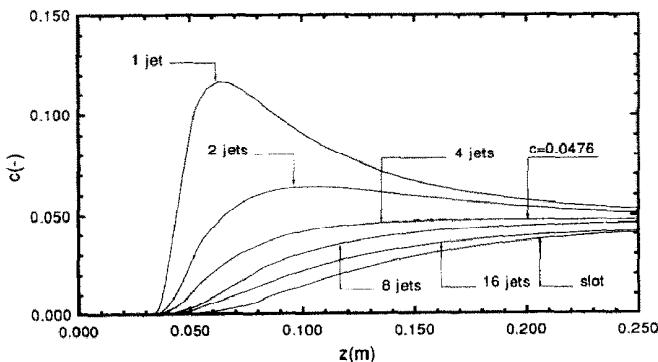


FIG. 6. Helium mass fraction profiles on the centerline of the plasma reactor.



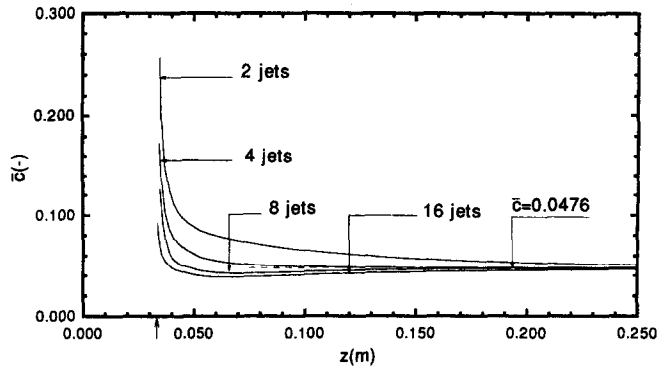


FIG. 7. Averaged helium mass fraction profiles along the plane of symmetry.

tion points, is presented in Figs. 4(a) and (b). These contours are similar in many aspects to those corresponding to the temperature distributions (Figs. 3(a) and (b)). The helium mass fraction contours obtained with these injection modes indicate that a better mixing is obtained with the two jets case. Figures 4(c) and (d) show the helium mass fraction obtained respectively with 4 and 8 jets. One can see that, in the 4 jets case, the injected gas mixes rapidly with the argon plasma stream; in this case the convection and molecular diffusion contribute significantly to the mixing, while for 8 jets case, the mixing process is controlled essentially by molecular diffusion phenomena. A comparison of helium mass fraction distributions in the plane of symmetry obtained with 16 jets and that for a slot is shown in Figs. 4(e) and (f). These figures show that the approximation of the 16 jets injection problem by a slot is acceptable. In comparison to the slot case (Fig. 4(f)), the 8 jets (Fig. 4(c)) and 16 jets (Fig. 4(e)) cases present some differences near the injection section, while farther downstream, the helium mass fraction contours are almost identical. For the studied cases, it is worth noticing from results presented in Fig. 4 that the jets spread in a multiple injection problem is a decreasing function of the number of injection points. Figure 4 also shows that as the number of jets increases, the jets are severely deflected and the region of helium concentration, i.e. containing origin jet fluid are found in the wake region attached to the wall.

The predicted temperature profiles in the plane of symmetry at one reactor diameter downstream of the injection section ( $z - z_i = 50$  mm) are presented in Fig. 5(a). Here again we notice different results between the different injection modes. This figure shows that the 2 jets injection mode is responsible for the faster cooling of the plasma flow. These profiles also show that the cooling effect decreases as the number of jets is increased. This is mainly due to the fact that convection plays a more important role in the mixing process for a smaller number of jets. The corresponding predicted helium mass fraction profiles are shown in Fig. 5(b). We notice that for eight or more injection ports the helium mass fraction profile

approaches that of a slot. This figure also shows that, near the injection section, the numerical treatment of a multiple injection problem by a 2-D model is inaccurate even for a relatively high number of jets.

Profiles of helium mass fraction on the centerline of the plasma reactor are presented in Fig. 6. These profiles indicate that injection with a single point exhibits a more pronounced penetration than injection using two or more injection ports. This figure underlines again the critical differences observed in the region close to the injection section where approximation of 1, 2 or 4 jets by a circular slot is definitively a poor hypothesis.

Finally, the variation of the averaged helium mass fraction along the plane of symmetry and downstream the injection section is shown in Fig. 7. This was calculated as follows:

$$\bar{c} = \frac{\int_{-R}^R c \, dy}{2R}. \quad (6)$$

The profiles obtained with 2, 4, 8, and 16 jets indicate that using a 4 points gas injection configuration leads, for the studied flow conditions, to a better mixing with the plasma stream.

#### 4. CONCLUSIONS

The following conclusions may be drawn from this study:

- A 3-D laminar model for the prediction of the mixing pattern between a single and multiple cold jets and a transverse plasma stream has been developed. The results show that in most cases, complete mixing of gaseous stream can be achieved within two tube diameters from the injection section. Faster mixing is achieved with a smaller number of injection ports (2 or 4) while the slowest mixing is achieved using the slot injection configuration.

- The results also show that simplification of 3-D mixing of cold jets with a transverse plasma flow by a 2-D model is quite acceptable from 8 or more injection

points; this approximation results, however, in a poor description of the mixing pattern near the injection section for a relatively reduced number of jets.

*Acknowledgements*—The financial support by the Natural Sciences and Engineering Research Council of Canada (NSERC) and by the Ministry of Education of the Province of Québec is gratefully acknowledged.

## REFERENCES

1. C. B. Laflamme, G. Soucy, J. W. Jurewicz and M. I. Boulos, Synthèse de poudres céramiques ultrafines par plasma, *J. High Temp. Chem. Proc.* **1**, 283–301 (1992).
2. G. Soucy, Synthèse de poudres ultrafines de Si<sub>3</sub>N<sub>4</sub> par plasma inductif, Ph.D. Thesis, Chemical Engineering Department, University of Sherbrooke, Sherbrooke, Québec, Canada (1992).
3. G. Soucy, J. W. Jurewicz and M. I. Boulos, Mixing study of the induction plasma reactor: part I. Axial injection mode, *J. Plasma Chem. Plasma Proc.*, in press.
4. G. Soucy, J. W. Jurewicz and M. I. Boulos, Mixing study of the induction plasma reactor: part II. Radial injection mode, *J. Plasma Chem. Plasma Proc.*, in press.
5. X. Chen, Y. C. Lee and E. Pfender, The importance of the Knudsen and evaporation effects on modelling in thermal plasma processing, *Proceedings of ISPC-6*, Montréal, Vol. 1, pp. 51–58 (1983).
6. R. Jordison, Flow in a jet directed normal to the wind, *British Aeronautical Research Council*, R&M 3074 (1956).
7. J. F. Keffer and W. D. Baines, The round turbulent jets in cross flow, *J. Fluid Mech.* **15**, 481–496 (1963).
8. J. F. Keffer, The physical nature of the subsonic jet in a cross-stream, Analysis of a Jet in a Subsonic Crosswind, NASA Technical Notes, SP-218, pp. 19–36 (1969).
9. J. L. Platten and J. F. Keffer, Deflected turbulent jet flows, *J. Appl. Mech.* **38**, 756–758 (1971).
10. Z. M. Moussa, J. W. Trischka and S. Eskinazi, The near field in the mixing of a round jet with a cross stream, *J. Fluid Mech.* **80**, 49–80 (1977).
11. M. A. Patrick, Experimental investigation of the mixing and penetration of a round turbulent jet injected perpendicularly into a traverse stream, *Trans. Instn Chem. Engrs* **45**, 16–31 (1967).
12. G. Gelb and W. Martin, An experimental investigation of the flow field about a subsonic jet exhausting into a quiescent and a low velocity air stream, *Can. Aero. Space J.* **12**, 333–342 (1966).
13. J. C. Wu, H. M. McMahon, D. K. Mosher and M. A. Wright, Experimental and analytical investigations of jets exhausting into a deflecting stream, *J. Aircraft* **7**, 44–51 (1970).
14. H. M. McMahon and D. K. Mosher, Experimental investigation of pressures induced on a flat plate by a jet issuing into a subsonic crosswind, Analysis of a Jet in a Subsonic Crosswind, NASA SP-218, pp. 49–62 (1969).
15. R. J. Margason, Jet-wake characteristics and their induced aerodynamic effects on V/STOL aircraft in transition flight, NASA SP-218, pp. 1–18 (1969).
16. H. M. McMahon, D. D. Hester and J. G. Palfery, Vortex shedding from a turbulent jet in a crosswind, *J. Fluid Mech.* **48**, 73–80 (1971).
17. W. T. Mikolowsky and H. M. McMahon, An experimental investigation of a jet issuing from wing in a cross flow, *J. Aircraft* **10**, 546–553 (1973).
18. J. W. Ramsey, The interaction of a heated air jet with a deflecting flow, Ph.D. Thesis, University of Minnesota, Minneapolis, Minnesota (1969).
19. J. W. Ramsey and R. J. Goldstein, Interaction of a heated jet with a deflecting stream, *J. Heat Transfer* **93**, 365–372 (1971).
20. J. F. Campbell and J. A. Schetz, Penetration and mixing of heated jets in a waterway with applications to the thermal pollution problem, AIAA paper No 71-524 (1971).
21. Y. Kamotani and I. Greber, Experiments on turbulent jet in a cross flow, *AIAA J.* **10**, 1425–1429 (1972).
22. G. Rudinger, Experimental investigation of gas injection through a transverse slot into a subsonic cross flow, *AIAA J.* **12**, 566–568 (1974).
23. P. Chassing, J. George, A. Claria and F. Sananes, Physical characteristics of subsonic jets in a cross stream, *J. Fluids Mech.* **62**, 41–65 (1974).
24. G. Bergeles, A. D. Gosman and B. E. Launder, The near field character of a jet discharged normal to a main stream, *J. Heat Transfer* **98**, 373–378 (1976).
25. D. Crabb, D. F. G. Durao and J. H. Whitelaw, A round jet normal to a cross flow, *J. Fluids Engng* **103**, 142–153 (1981).
26. N. Rajaratnam and T. Gangadharaiyah, Entrainment by circular jets in cross flow, *J. Wind Engng Ind. Aerodynamics* **9**, 251–255 (1982).
27. J. Andreopoulos, Measurements in a pipe flow issuing perpendicularly into a cross stream, *J. Fluids Engng* **104**, 493–499 (1982).
28. J. Andreopoulos, Heat transfer measurements in a heated jet-pipe flow issuing into a cold cross-stream, *Phys. Fluids* **26**, 3201–3210 (1983).
29. J. Andreopoulos, On the structure of jets in a cross flow, *J. Fluid Mech.* **157**, 163–179 (1985).
30. S. A. Sherif and R. H. Pletcher, Measurements of the flow and turbulence characteristics of round jets in cross flow, *J. Fluids Engng* **111**, 165–171 (1989).
31. S. A. Sherif and R. H. Pletcher, Measurements of the thermal characteristics of heated turbulent jets in cross flow, *J. Heat Transfer* **111**, 897–903 (1989).
32. S. A. Sherif and R. H. Pletcher, Jet-wake thermal characteristics of heated turbulent in cross flow, *J. Thermophys. Heat Transfer* **5**, 181–191 (1991).
33. J. L. Platten and J. F. Keffer, Entrainment in deflected axisymmetric jets at various angles to the stream, Mechanical Engineering Rept. TP-6808, University of Toronto, Ontario, Canada (1968).
34. H. Ziegler and P. T. Wooler, Multiple jets exhausting into a cross flow, *J. Aircraft* **8**, 414–420 (1971).
35. J. H. Kim, An analytical model for the buoyant jet injected into pipe flow, *J. Heat Transfer* **107**, 630–635 (1985).
36. A. R. Karagozian, An analytical model for the vorticity associated with a transverse jet, *AIAA J.* **24**, 429–436 (1986).
37. J. C. Chien and J. A. Schetz, Numerical solution of three-dimensional Navier–Stokes equations with applications to channel flows and a buoyant jet in a cross flow, *J. Appl. Mech.* **42**, 575–579 (1975).
38. S. V. Patankar, D. K. Basu and S. A. Alpay, Prediction of the 3-dimensional velocity field of a turbulent deflected jet, *J. Fluids Engng* **99**, 758–762 (1977).
39. G. Bergeles, A. D. Gosman and B. E. Launder, The turbulent jet in a cross stream at low injection rates: a three-dimensional numerical treatment, *Numer. Heat Transfer* **1**, 217–242 (1978).
40. A. O. Demuren, Numerical calculations of steady 3-dimensional turbulent jets in cross flow, *Comput. Meth. Appl. Mech. Engng* **37**, 309–328 (1982).
41. J. Mostaghimi, P. Proulx and M. I. Boulos, Parametric study of the flow and temperature fields in an inductively coupled r.f. plasma torch, *Plasma Chem. Plasma Proc.* **4**, 199–217 (1984).
42. J. Mostaghimi, P. Proulx and M. I. Boulos, An analysis of the computer modeling of the flow and temperature fields in an inductively coupled plasma, *Numer. Heat Transfer* **8**, 187–201 (1985).

43. M. I. Boulos, J. T. Mostaghimi and P. Proulx, High frequency induction plasma: HiFi computer code, Chemical Engineering Department, University of Sherbrooke, Québec, Canada (1989).
44. R. Bird, W. E. Stewart and E. N. Lightfoot, *Transport Phenomena*, p. 780. Wiley, New York (1960).
45. S. V. Patankar, *Numerical Heat Transfer and Fluid Flow*, p. 197. McGraw-Hill, New York (1980).
46. Z. Njah, J. Mostaghimi, M. Faghri and M. Boulos, Study of 3-D mixing of a cold jet with a transverse plasma stream, *Int. J. Heat Mass Transfer* **36**, 3897–3907 (1993).